INTERNATIONAL JOURNAL FOR NUMERICAL AND ANALYTICAL METHODS IN GEOMECHANICS
Preprint: Accepted for publication

A hypoplastic constitutive model for clays

D. Mašín[1*†]

[1] *Institute of Hydrogeology, Engineering Geology and Applied Geophysics, Charles University, Albertov 6, 128 43 Prague 2, Czech Republic*

SUMMARY

This paper presents a new constitutive model for clays. The model is developed on the basis of generalised hypoplasticity principles, which are combined with traditional critical state soil mechanics. The positions of the isotropic normal compression line and the critical state line correspond to the Modified Cam clay model, the Matsuoka–Nakai failure surface is taken as the limit stress criterion and the nonlinear behaviour of soils with different overconsolidation ratios is governed by the generalised hypoplastic formulation.

The model requires five constitutive parameters, which correspond to the parameters of the Modified Cam clay model and are simple to calibrate on the basis of standard laboratory experiments. This makes the model particularly suitable for practical applications. The basic model may be simply enhanced by the intergranular strain concept, which allows reproducing the behaviour at very small strains. The model is evaluated on the basis of high quality laboratory experiments on reconstituted London clay. Contrary to a reference hypoplastic relation, the proposed model may be applied to highly overconsolidated clays. Improvement of predictions in the small strain range at different stress levels is also demonstrated. Copyright © 2004 John Wiley & Sons, Ltd.

KEY WORDS: clay; constitutive model; hypoplasticity

1. INTRODUCTION

In the past years many constitutive models based on the theory of hypoplasticity [21] have been developed for granular materials. This research, traced in Sec. 2.1, has led to constitutive equations that can take into account the nonlinearity of the soil behaviour, the influence of barotropy and pyknotropy and also the behaviour at small to very small strains with the influence of the recent history of deformation [32].

The research into hypoplasticity, based at the University of Karlsruhe, was mainly focused on the development of constitutive models for granular materials, such as sands or gravels. An

*Correspondence to: David Mašín, Institute of Hydrogeology, Engineering Geology and Applied Geophysics, Charles University, Albertov 6, 128 43 Prague 2, Czech Republic
†E-mail: masin@natur.cuni.cz, Tel: +420-2-2195 1552, Fax: +420-2-2195 1556

Contract/grant sponsor: Grant Agency of the Czech Republic; contract/grant number: 205/03/1467

important example is the model by von Wolffersdorff [43] (referred to in the following text "VW model"), which can be considered as a synthesis of the research work carried out in Karlsruhe[†] on this subject. Only a few attempts however have been made to apply hypoplastic principles to fine grained soils. A notable example are the visco–hypoplastic models by Niemunis [30, 33, 31]. These models assume logarithmic compression law [2] and, in line with the critical state soil mechanics [37], the lower limit for the void ratio e is equal to 0. Their formulation however concentrates on prediction of viscous effects and, since they arise from the model by von Wolffersdorff [43], it is not possible to specify the shear stiffness independently of the bulk stiffness and, as discussed by Herle and Kolymbas [14], the shear stiffness is significantly underpredicted.

A modification of the VW model, which allows for an independent calibration of the shear and bulk stiffnesses, was proposed by Herle and Kolymbas [14] (referred to in the following as the "HK model"). In the HK model, Herle and Kolymbas modified the hypoelastic tensor $\boldsymbol{\mathcal{L}}$ (Sec. 2.1), which was responsible for the too low shear stiffness predicted by the VW model for soils with low friction angles, and introduced an additional model parameter r controlling the ratio of shear and bulk moduli. This model however assumes the influence of the barotropy and pyknotropy identical to the VW model, which is not suitable for clays. Moreover, the modification of the tensor $\boldsymbol{\mathcal{L}}$ must vanish as the stress approaches the limit state, which leads to incorrect predictions of the shear stiffness for anisotropic stress states (for further discussion see Sec. 3). The lack of a suitable hypoplastic formulation for fine grained soils led to the development of the model proposed in this paper.

In the following, the usual sign convention of solid mechanics (compression negative) is adopted throughout, except Roscoe's variables p, q, ϵ_v and ϵ_s (e.g. [29]), which are defined positive in compression. In line with the Terzaghi principle of effective stress, all stresses are *effective* stresses. Second–order tensors are denoted with bold letters (e.g., $\mathbf{T}$, $\mathbf{m}$) and fourth–order tensors with calligraphic bold letters (e.g., $\boldsymbol{\mathcal{L}}$). Different types of tensorial multiplication are used: $\mathbf{T} \otimes \mathbf{D} = \mathrm{T}_{ij}\mathrm{D}_{kl}$, $\mathbf{T} : \mathbf{D} = \mathrm{T}_{ij}\mathrm{D}_{ij}$, $\boldsymbol{\mathcal{L}} : \mathbf{D} = \mathcal{L}_{ijkl}\mathrm{D}_{kl}$, $\mathbf{T} \cdot \mathbf{D} = \mathrm{T}_{ij}\mathrm{D}_{jk}$. The quantity $\|\mathbf{X}\| = \sqrt{\mathbf{X} : \mathbf{X}}$ denotes the Euclidean norm of $\mathbf{X}$, the operator arrow is defined as $\vec{\mathbf{X}} = \mathbf{X}/\|\mathbf{X}\|$ and trace by $\mathrm{tr}\mathbf{X} = \mathbf{X} : \mathbf{1}$. $\mathbf{1}$ is a second–order unity tensor and $\boldsymbol{\mathcal{I}}$ is a fourth order unity tensor with components $\mathcal{I}_{ijkl} = \frac{1}{2}\left(1_{ik}1_{jl} + 1_{il}1_{jk}\right)$.

2. HYPOPLASTICITY

2.1. General aspects

The hypoplastic constitutive equations are usually described by a simple non–linear tensorial equation that relates the objective (Jaumann) stress rate $\mathring{\mathbf{T}}$ with the Euler's stretching tensor $\mathbf{D}$.

The early hypoplastic models were developed by trial and error, by choosing suitable candidate functions (Kolymbas [19]) from the most general form of isotropic tensor–valued functions of two tensorial arguments (representation theorem due to Wang [42]). The suitable

[†]There is also the second school of thought in the research on incrementally nonlinear models, Grenoble (e.g., [6]). This article however focuses on the developments of the German school.

candidate functions were combined automatically using a computer program that tested the capability of the constitutive model to predict the most important aspects of the soil behaviour [20]. The research led to a practically useful equation with four parameters proposed by Wu [45] and Wu and Bauer [46].

As proven in [23], the hypoplastic equation may be written in its general form as

$$\mathring{\mathbf{T}} = \boldsymbol{\mathcal{L}} : \mathbf{D} + \mathbf{N}\|\mathbf{D}\|, \tag{1}$$

where $\boldsymbol{\mathcal{L}}$ and $\mathbf{N}$ are fourth and second–order constitutive tensors respectively that are functions of the Cauchy stress $\mathbf{T}$ only in the case of early hypoplastic models.

An important step forward in developing the hypoplastic model was the implementation of the critical state concept. Gudehus [13] proposed a modification of Eq. (1) to include the influence of the stress level (barotropy) and the influence of density (pyknotropy). The modified equation reads

$$\mathring{\mathbf{T}} = f_s \boldsymbol{\mathcal{L}} : \mathbf{D} + f_s f_d \mathbf{N}\|\mathbf{D}\|. \tag{2}$$

Here f_s and f_d are scalar factors expressing the influence of barotropy and pyknotropy. The model [13] was later refined by von Wolffersdorff [43] to incorporate Matsuoka–Nakai critical state stress condition.

A successful modification of the VW model is not straightforward due to the fact that the constitutive tensors $\boldsymbol{\mathcal{L}}$ and $\mathbf{N}$ are interrelated – they act together as a hypoplastic flow rule and limit stress condition. To overcome this problem, it is convenient to introduce the tensorial function

$$\mathbf{B} = \boldsymbol{\mathcal{L}}^{-1} : \mathbf{N}, \tag{3}$$

which has been already used in the development of both Karlsruhe hypoplastic models [20] and CLoE hypoplastic models [6]. The Eq. (2) may be re–written,

$$\mathring{\mathbf{T}} = f_s \boldsymbol{\mathcal{L}} : (\mathbf{D} + f_d \mathbf{B}\|\mathbf{D}\|)\,. \tag{4}$$

The critical state condition can be found by substituting $\mathring{\mathbf{T}} = \mathbf{0}$ and $f_d = 1$ into (4). It follows that $\mathring{\mathbf{T}} = \mathbf{0}$ is satisfied trivially by $\mathbf{D} = \mathbf{0}$ and for $\mathbf{D} \neq \mathbf{0}$ by

$$\vec{\mathbf{D}} = -\mathbf{B}. \tag{5}$$

Eq. (5) imposes a condition on stress, which can be revealed by elimination of $\vec{\mathbf{D}}$ from (5). Taking the norm of both sides of (5) we obtain for the critical state

$$f = \|\mathbf{B}\| - 1 = 0. \tag{6}$$

The stress function f may be seen as a counterpart of the critical state stress criterion in elasto–plasticity [19]. A hypoplastic flow rule is then given by Eq. (5).

Using these transformations, Niemunis [31] proposed a simple rearrangement of the basic hypoplastic equation (2), which allows definition of the flow rule, critical state stress condition and tensor $\boldsymbol{\mathcal{L}}$ independently. Such a rearrangement is useful for model development and will also be used in this work.

The second–order tensor $\mathbf{N}$ is now calculated by

$$\mathbf{N} = \boldsymbol{\mathcal{L}} : \left(-Y \frac{\mathbf{m}}{\|\mathbf{m}\|}\right). \tag{7}$$

Here the scalar quantity $Y = f + 1$ (named the *degree of nonlinearity* [31]) stands for a limit stress condition, $\mathbf{m}$ is a second–order tensor denoted hypoplastic flow rule and $\boldsymbol{\mathcal{L}}$ is a fourth–order hypoelastic tensor from Eq. (2).

Eqs. (2) and (7) can be combined to get

$$\mathring{\mathbf{T}} = f_s \boldsymbol{\mathcal{L}} : \left(\mathbf{D} - f_d Y \frac{\mathbf{m}}{\|\mathbf{m}\|} \|\mathbf{D}\| \right). \tag{8}$$

Eqs. (2) and (7), or Eq. (8), define the general stress–strain relationship of the model proposed. Following [31], this formulation is named "generalised hypoplasticity".

2.2. Reference constitutive model

The HK model, introduced in Sec. 1, is taken as a reference model for the present research and its mathematical formulation is summarised in Appendix A. The tensor $\boldsymbol{\mathcal{L}}$ of the VW model is modified by introducing two scalar factors c_1 and c_2,

$$\boldsymbol{\mathcal{L}} = \frac{1}{\hat{\mathbf{T}} : \hat{\mathbf{T}}} \left(c_1 F^2 \boldsymbol{\mathcal{I}} + c_2 a^2 \hat{\mathbf{T}} \otimes \hat{\mathbf{T}} \right), \tag{9}$$

where quantities $\hat{\mathbf{T}}$, F and a are defined in Appendix A. The expression for the factor c_1 is derived in order to ensure that the additional model parameter r specifies the ratio of the bulk and shear moduli at isotropic stress state (details are given in Sec. 4.6) and factor c_2 follows from the requirement that the isotropic formulations of both the HK and VW models merge,

$$c_1 = \left(\frac{1 + \frac{1}{3}a^2 - \frac{1}{\sqrt{3}}a}{1.5r} \right)^{\xi}, \qquad c_2 = 1 + (1 - c_1)\frac{3}{a^2}. \tag{10}$$

Because the HK model does not make use of the generalised hypoplasticity formulation (Sec. 2.1), the influence of fators c_1 and c_2 must vanish as the stress approaches Matsuoka–Nakai critical state stress criterion. For this reason, a scalar factor ξ is introduced in the formulation of the factor c_1 (Eq. (10)), which reads

$$\xi = \left\langle \frac{\sin\varphi_c - \sin\varphi_{mob}}{\sin\varphi_c} \right\rangle, \qquad \text{where} \qquad \sin\varphi_{mob} = \frac{T_1 - T_3}{T_1 + T_3}. \tag{11}$$

T_1 and T_3 are the maximal and minimal principal stresses, φ_{mob} is a mobilized friction angle and $\langle\rangle$ are Macauley brackets: $\langle x \rangle = (x + |x|)/2$.

2.3. Intergranular strain concept

The hypoplastic models discussed in previous sections are capable of predicting the soil behavior upon monotonic loading at medium to large strain levels. In order to prevent excessive ratcheting upon cyclic loading and to improve model performance in the small–strain range, the mathematical formulation has been enhanced by the intergranular strain concept [32].

The rate formulation of the enhanced model is given by

$$\mathring{\mathbf{T}} = \boldsymbol{\mathcal{M}} : \mathbf{D}, \tag{12}$$

where $\boldsymbol{\mathcal{M}}$ is the fourth–order tangent stiffness tensor of the material. The formulation introduces the additional state variable $\boldsymbol{\delta}$, which is a symmetric second order tensor called *intergranular strain*.

In the formulation described above, the total strain can be thought of as the sum of a component related to the deformation of interface layers at integranular contacts, quantified by $\boldsymbol{\delta}$, and a component related to the rearrangement of the soil skeleton. For reverse loading conditions ($\hat{\boldsymbol{\delta}} : \mathbf{D} < 0$, where $\hat{\boldsymbol{\delta}}$ is defined in Appendix B) and neutral loading conditions ($\hat{\boldsymbol{\delta}} : \mathbf{D} = 0$), the observed overall strain is related only to the deformation of the intergranular interface layer and the soil behaviour is hypoelastic, whereas in continuous loading conditions ($\hat{\boldsymbol{\delta}} : \mathbf{D} > 0$) the observed overall response is also affected by particle rearrangement in the soil skeleton. From the mathematical standpoint, the response of the model is determined by interpolating between the following three special cases:

$$\begin{array}{lll} \mathring{\mathbf{T}} = m_R f_s \boldsymbol{\mathcal{L}} : \mathbf{D}, & \text{for} & \hat{\boldsymbol{\delta}} : \mathbf{D} = -1 \text{ and } \boldsymbol{\delta} = \mathbf{0}; \\ \mathring{\mathbf{T}} = m_T f_s \boldsymbol{\mathcal{L}} : \mathbf{D}, & \text{for} & \hat{\boldsymbol{\delta}} : \mathbf{D} = 0; \\ \mathring{\mathbf{T}} = f_s \boldsymbol{\mathcal{L}} : \mathbf{D} + f_s f_d \mathbf{N} \|\mathbf{D}\|, & \text{for} & \hat{\boldsymbol{\delta}} : \mathbf{D} = 1. \end{array} \tag{13}$$

Full details of the mathematical structure of the model are provided in Appendix B. The model, which incorporates the intergranular strain concept is in the paper denoted as "enhanced", the model without this modification as "basic".

3. LIMITATIONS OF THE REFERENCE MODEL

As pointed out in the introduction, although the HK model improved predictions of the clay behaviour significantly, several shortcomings may still be identified. The most important are:

- Measurements of the shear stiffness at very small strains (G_0), by means of propagation of shear waves, allows investigation of the dependence of G_0 on the stress level. For clays such studies were performed for example in [41, 17, 40, 4]. It was shown that for stresses inside the limit state surface G_0 depends on the mean stress p but the influence of the deviatoric stress q is not significant (both for triaxial compression and extension). The HK model with intergranular strains however predicts significant decrease of the hypoelastic shear modulus G_0 with the ratio $\eta = q/p$, as discussed in Sec. 5 (Figs. 3 and 4).
- The HK model assumes a non–zero, pressure–dependent lower limit of void ratio, e_d. While this approach is suitable for granular materials, for clays it is reasonable to consider the lower limit of void ratio of $e = 0$, according to the critical state soil mechanics [37], supported by experimental studies on the shape of the state boundary surface of fine–grained soils (e.g., [7, 8, 9]). Taking the pyknotropy factor f_d a function of relative density r_e calculated by
$$r_e = \frac{e - e_d}{e_c - e_d}, \tag{14}$$
with e_c being void ratio at the critical state line at current mean stress, leads to incorrect predictions of the stress–dilatancy behaviour by the HK model (for details see Sec. 5, Fig. 6), also for the case when lower limit of void ratio $e = 0$ is prescribed ($e_{d0} = 0$).
- The HK model adopts exponential expressions for the isotropic normal compression and critical state lines [1]. Compared to the logarithmic expression, the exponential expression has the advantage of having limits for $p \to 0$ and $p \to \infty$. For clays however

the logarithmic expression is more accurate in the stress range applicable in geotechnical engineering [2], with the further advantage of having one material parameter less.
- Taking into account the desired simplicity of the calibration of the proposed model, the parameter defining the position of the critical state line in the $e : p$ plane (e_{c0}) may be regarded as superfluous. For clays the position of the critical state line calculated using the state boundary surface of the Modified Cam clay model [36] is sufficiently accurate, as shown recently for different clays in [7, 8, 9].
- The HK model does not allow specifying directly the swelling index, κ^*. The slope of the isotropic unloading line is governed by two parameters, α and β. Direct evaluation of these parameters from isotropic unloading test is complicated and the calibration is usually performed by means of a parametric study.

The proposed hypoplastic model for clays aims at overcoming the outlined shortcomings of the HK model and achieving maximal simplicity of the calibration of the new model, which is desired in practical applications.

4. PROPOSED CONSTITUTIVE MODEL

4.1. Tensor $\boldsymbol{\mathcal{L}}$

The tensor $\boldsymbol{\mathcal{L}}$ (Eq. (9)) determines, in the model enhanced by the intergranular strain concept (Sec. 2.3), the initial hypoelastic stiffness and causes the HK model to predict a decrease of the initial shear modulus G_0 with the stress ratio η, which is not in agreement with experiment (see Sec. 3). The influence of η on G_0 is caused by the factor $1/(\hat{\mathbf{T}} : \hat{\mathbf{T}})$ (where $\hat{\mathbf{T}} = \mathbf{T}/\mathrm{tr}\mathbf{T}$), the decrease of the scalar quantity ξ as the stress approaches limit state and the factor F, which increases the compressibility for Lode angles different than $\pi/6$.

The influence of the first two factors is studied using the concept of incremental response envelopes [39]. This concept follows directly from the concept of rate response envelope [12], with rates replaced by finite–size increments with *constant* direction of stretching $\vec{\mathbf{D}}$ (for brevity, incremental response envelopes are referred to as response envelopes in this work). Response envelopes are plotted for $\Delta t\|\mathbf{D}\| = 0.0015$, where t is pseudo–time used for time integration of the model response. The HK model enhanced by the intergranular strain concept is used in the simulations, modified by either keeping $1/(\hat{\mathbf{T}} : \hat{\mathbf{T}}) = \text{const.} = 3$ or $\eta = \text{const.} = 1$ (Fig. 1). The initial value of the intergranular strain tensor $\boldsymbol{\delta}$ is equal to $\mathbf{0}$.

It may be seen From Fig. 1 (left) that the influence of the stress quantity $1/(\hat{\mathbf{T}} : \hat{\mathbf{T}})$ is not significant. In the VW model this quantity was introduced in order to emphasize that the overall compressibility of sand is larger at higher stress ratios. For clays it is well known that the normal compression lines are approximately parallel for different radial stress paths (as isotropic and K_0 normal compression lines and critical state line). Following Niemunis [31], the factor $1/(\hat{\mathbf{T}} : \hat{\mathbf{T}})$ may be disregarded and in the present model it is replaced by its isotropic value equal to 3.

Fig. 1 (right) shows that the influence of the factor ξ, which in the HK model must decrease with φ_{mob} in order to ensure that the model predicts correctly the critical state (Sec. 2.2), is very significant. The response envelopes become narrower as the stress approaches the critical state and the initial shear modulus G_0 decreases significantly. The proposed model therefore

Preprint: Accepted for publication

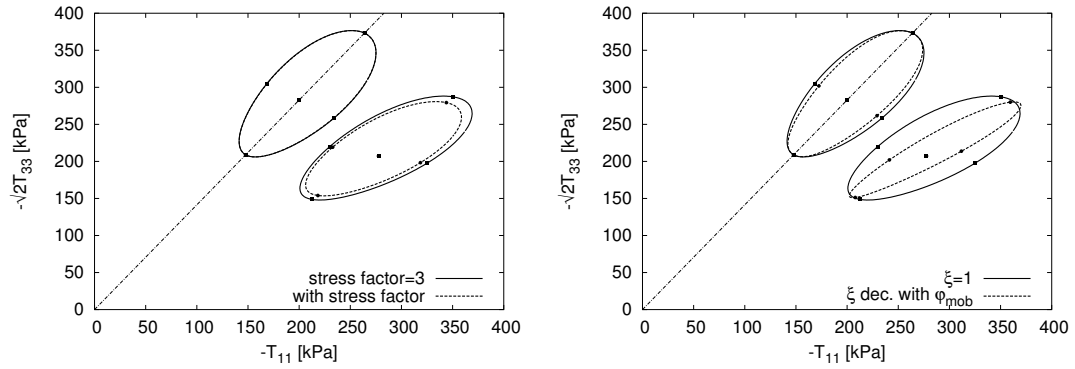

Figure 1. The influence of the stress factor $1/(\hat{\mathbf{T}} : \hat{\mathbf{T}})$ (left) and the scalar quantity ξ (right) in the expression for $\boldsymbol{\mathcal{L}}$ on the size and shape of response envelopes.

does not make use of the quantity ξ and so constant values of scalar factors c_1 and c_2 (Sec. 2.2) are assumed. This modification is enabled by adopting the generalised hypoplastic formulation (Sec. 2.1).

In the VW model the factor F had to enter the expression for $\boldsymbol{\mathcal{L}}$ to ensure that the function $\mathbf{B}$ conforms with the Matsuoka–Nakai failure criterion. As quoted in Sec. 3, according to experiments on fine–grained soils, G_0 is independent of η in both triaxial compression and extension [41]. Therefore, the factor F should be in the expression for $\boldsymbol{\mathcal{L}}$ omitted.

We assume the following formulation of the hypoelastic tensor $\boldsymbol{\mathcal{L}}$:

$$\boldsymbol{\mathcal{L}} = 3\left(c_1\boldsymbol{\mathcal{I}} + c_2 a^2 \hat{\mathbf{T}} \otimes \hat{\mathbf{T}}\right). \tag{15}$$

The calculation of scalar factors c_1 and c_2, which follows [14], is described in Sec. 4.6. The scalar factor a is a function of material parameter φ_c and follows from VW model,

$$a = \frac{\sqrt{3}\,(3 - \sin\varphi_c)}{2\sqrt{2}\sin\varphi_c}. \tag{16}$$

4.2. Limit stress condition Y

As shown, for example, in [18, 3, 35] the Drucker–Prager critical state stress criterion, which is assumed also by the Modified Cam clay model, is not suitable for clays. The actual critical state stress criterion circumscribes the Mohr–Coulomb criterion with approximately equal friction angles in triaxial compression and extension.

Therefore, the Matsuoka–Nakai [24] criterion assumed by the VW hypoplastic model is applicable also for clays. It is described by the equation

$$f = -\frac{I_1 I_2}{I_3} - \frac{9 - \sin^2\varphi_c}{1 - \sin^2\varphi_c} \leq 0, \tag{17}$$

with the stress invariants

$$I_1 = \mathrm{tr}\mathbf{T}, \qquad I_2 = \frac{1}{2}\left[\mathbf{T} : \mathbf{T} - (I_1)^2\right], \qquad I_3 = \det\mathbf{T}. \tag{18}$$

As pointed out by Niemunis [31], the quantity Y should have a minimum value at the isotropic axis (maximum $Y = 1$ at the critical state stress criterion). Direct linear interpolation between the isotropic value $Y = Y_i$ and limit state value $Y = 1$ is assumed in the proposed model, following [31].

Using the fact that $I_1 I_2 / I_3 = -9$ at the hydrostatic stress state, the linear interpolation reads

$$Y = (1 - Y_i) \left[\frac{-\dfrac{I_1 I_2}{I_3} - 9}{\dfrac{9 - \sin^2 \varphi_c}{1 - \sin^2 \varphi_c} - 9} \right] + Y_i, \tag{19}$$

with Y_i being equal to the isotropic value of the function $\|\mathbf{B}\|$ of the VW (HK) model,

$$Y_i = \frac{\sqrt{3} a}{3 + a^2}. \tag{20}$$

4.3. Hypoplastic flow rule (tensorial quantity $\mathbf{m}$*)*

$\vec{\mathbf{m}} = \mathbf{m}/\|\mathbf{m}\|$ is a tensorial function that should have purely volumetric direction at isotropic stress state and purely deviatoric direction (tr $\mathbf{m} = 0$) at Matsuoka–Nakai states,

$$\begin{cases} \vec{\mathbf{m}} = -\hat{\mathbf{T}}^* / \|\hat{\mathbf{T}}^*\|, & \text{for} \quad Y = 1; \\ \vec{\mathbf{m}} = -\frac{1}{\sqrt{3}} \mathbf{1}, & \text{for} \quad Y = Y_i, \end{cases} \tag{21}$$

where the stress quantity $\hat{\mathbf{T}}^*$ is defined as $\hat{\mathbf{T}}^* = \hat{\mathbf{T}} - \mathbf{1}/3$. A suitable candidate is the function $-\mathbf{B}$ of the VW hypoplastic model [43],

$$\mathbf{m} = -\frac{a}{F} \left[\hat{\mathbf{T}} + \hat{\mathbf{T}}^* - \frac{\hat{\mathbf{T}}}{3} \left(\frac{6\ \hat{\mathbf{T}} : \hat{\mathbf{T}} - 1}{(F/a)^2 + \hat{\mathbf{T}} : \hat{\mathbf{T}}} \right) \right], \tag{22}$$

with factor F defined by

$$F = \sqrt{\frac{1}{8} \tan^2 \psi + \frac{2 - \tan^2 \psi}{2 + \sqrt{2} \tan \psi \cos 3\theta}} - \frac{1}{2\sqrt{2}} \tan \psi, \tag{23}$$

where

$$\tan \psi = \sqrt{3} \|\hat{\mathbf{T}}^*\|, \qquad \cos 3\theta = -\sqrt{6} \frac{\mathrm{tr} \left(\hat{\mathbf{T}}^* \cdot \hat{\mathbf{T}}^* \cdot \hat{\mathbf{T}}^* \right)}{\left[\hat{\mathbf{T}}^* : \hat{\mathbf{T}}^* \right]^{3/2}}. \tag{24}$$

Note that the adopted formulation of the function $\mathbf{m}$ implies radial strain increments in octahedral plane at the critical state. For fine–grained soils this choice is supported by the experimental evidence given by Kirkgard and Lade [18].

4.4. Barotropy factor f_s

The aim of the barotropy factor f_s is to incorporate the influence of the mean stress $p = -\mathrm{tr}\mathbf{T}/3$. The calculation of the factor f_s is based on the formulation of the pre–defined isotropic normal compression line.

The proposed model assumes isotropic normal compression line linear in the $\ln(1+e) : \ln p$ space, which is suitable for clays [2]. Its position is governed by the parameter N and its slope by the parameter λ^*,

$$\ln(1+e) = N - \lambda^* \ln p. \tag{25}$$

Time differentiation of (25) results in

$$\frac{\dot{e}}{1+e} = -\frac{\lambda^*}{p}\dot{p}. \tag{26}$$

The already defined quantities $\boldsymbol{\mathcal{L}}$, $\mathbf{m}$ and Y, together with the yet unknown values of pyknotropy factor f_d at the isotropic normally compressed state (f_{di}) and the factors c_1 and c_2, may be used to derive the form of the Eq. (7) for isotropic stress state. With the use of

$$\dot{p} = -\frac{1}{3}\mathrm{tr}\mathring{\mathbf{T}}, \quad \mathbf{D} = \frac{\dot{e}}{3\,(1+e)}\mathbf{1}, \quad \text{and} \quad \|\mathbf{D}\| = \frac{|\dot{e}|}{3\,(1+e)}\sqrt{3}, \tag{27}$$

we find

$$\dot{p} = -\frac{f_s}{3\,(1+e)}\left(3c_1 + a^2 c_2\right)\left[\dot{e} + f_{di}\frac{a\sqrt{3}}{3+a^2}|\dot{e}|\right]. \tag{28}$$

As discussed in Sec. 2.2, calculation of the scalar factor c_2, introduced in [14], ensures that the modification of the tensor $\boldsymbol{\mathcal{L}}$ does not influence the isotropic formulation of the model. Therefore it follows from (28) that

$$3c_1 + a^2 c_2 = 3 + a^2. \tag{29}$$

Eq. (28) may be therefore simplified to

$$\dot{p} = -\frac{1}{3\,(1+e)}f_s\left[\left(3+a^2\right)\dot{e} + f_{di}a\sqrt{3}|\dot{e}|\right], \tag{30}$$

and for isotropic compression with $\dot{e} < 0$

$$\dot{p} = -\left[\frac{1}{3\,(1+e)}f_s\left(3 + a^2 - f_{di}a\sqrt{3}\right)\right]\dot{e}. \tag{31}$$

Comparing (26) with (31) we derive the expression for the barotropy factor f_s,

$$f_s = -\frac{\mathrm{tr}\mathbf{T}}{\lambda^*}\left(3 + a^2 - f_{di}a\sqrt{3}\right)^{-1}. \tag{32}$$

4.5. Pyknotropy factor f_d

The pyknotropy factor f_d was introduced in [13] in order to incorporate the influence of density (overconsolidation ratio) on the soil behaviour. If we assume, following discussion in Sec. 3, that the lower limit of void ratio is $e = 0$ for clays, the pyknotropy factor f_d has the following properties:

- $f_d = 0$ for $p = 0$;
- $f_d = 1$ at the critical state;
- $f_d = \text{const.} > 1$ at isotropic normally compressed states.

Moreover, the pyknotropy factor f_d should have constant value along any other normal compression line (reasons for this choice are demonstrated in [26]). Taking into account the outlined properties of the factor f_d, we propose a simple expression

$$f_d = \left(\frac{p}{p_{cr}} \right)^{\alpha}, \tag{33}$$

where p_{cr} is the mean stress at the critical state line at the current void ratio (Fig. 2).

As discussed in Section 3, the position of the critical state line in $\ln(1+e) : \ln p$ space does not need to be controlled by an additional parameter, since for clays this position is sufficiently accurately defined by the state boundary surface of the Modified Cam clay model. The expression for the critical state line reads

$$\ln(1+e) = N - \lambda^* \ln 2 \frac{p_{cr}}{p_r}, \tag{34}$$

where p_r is the reference stress 1 kPa. Therefore,

$$f_d = \left[- \frac{2\mathrm{tr}\mathbf{T}}{3p_r} \exp\left(\frac{\ln(1+e) - N}{\lambda^*} \right) \right]^{\alpha}. \tag{35}$$

The scalar quantity α is calculated to allow for a direct calibration of the swelling index κ^*, defined as the slope of the isotropic unloading line in the $\ln(1+e) : \ln p$ space. This line has the expression

$$\ln(1+e) = \text{const.} - \kappa^* \ln p, \tag{36}$$

which leads after time differentiation to

$$\frac{\dot{e}}{1+e} = - \frac{\kappa^*}{p} \dot{p}. \tag{37}$$

For isotropic unloading from the isotropic *normally compressed* state the proposed model has the form (from Eq. (30))

$$\dot{p} = - \left[\frac{1}{3(1+e)} f_s \left(3 + a^2 + f_{di} a \sqrt{3} \right) \right] \dot{e}. \tag{38}$$

Having defined the barotropy factor f_s (32) and the pyknotropy factor for the isotropic normally compressed state f_{di} (from Eqs. (35) and (25)),

$$f_{di} = 2^{\alpha}, \tag{39}$$

we may rewrite Eq. (38) to get

$$\dot{p} = - \left[\frac{p}{\lambda^*(1+e)} \left(\frac{3 + a^2 + 2^{\alpha} a \sqrt{3}}{3 + a^2 - 2^{\alpha} a \sqrt{3}} \right) \right] \dot{e}. \tag{40}$$

Comparing (40) with (37) we derive the expression for the scalar quantity α,

$$\alpha = \frac{1}{\ln 2} \ln \left[\frac{\lambda^* - \kappa^*}{\lambda^* + \kappa^*} \left(\frac{3 + a^2}{a\sqrt{3}} \right) \right]. \tag{41}$$

The meaning of the model parameters N, λ^* and κ^* is demonstrated in Fig. 2.

Preprint: Accepted for publication

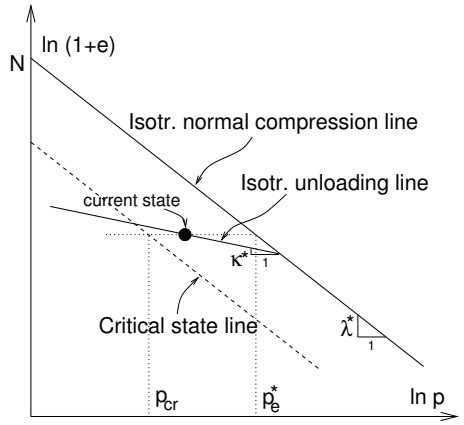

Figure 2. Definition of parameters N, λ^* and κ^* and quantities p_{cr} and p_e^* (from Sec. 5).

4.6. Scalar factors c_1 and c_2

Calculation of the factor c_2 is based on Eq. (29) and follows [14],

$$c_2 = 1 + (1 - c_1)\frac{3}{a^2}. \tag{42}$$

For the calculation of the factor c_1, we define the constitutive parameter r as the ratio of the bulk modulus in isotropic compression (K_i) and the shear modulus in undrained shear (G_i) for tests starting from the isotropic normally compressed state. Manipulation with the proposed model leads to expressions for K_i and G_i,

$$K_i = \frac{f_s}{3}\left(3 + a^2 - 2^\alpha a\sqrt{3}\right), \tag{43}$$

$$G_i = \frac{3}{2} f_s c_1. \tag{44}$$

Because $r = K_i/G_i$, we find

$$c_1 = \frac{2\left(3 + a^2 - 2^\alpha a\sqrt{3}\right)}{9r}. \tag{45}$$

Having obtained factors c_1 and c_2, the mathematical formulation of the proposed model is complete. It is summarized in Appendix C. The model requires five constitutive parameters: φ_c, λ^*, κ^*, N and r.

5. INSPECTION INTO PROPERTIES OF THE MODEL

5.1. Shear moduli

A significant shortcoming of the HK model is the underprediction of the initial shear stiffness G_0 for tests starting from anisotropic stress states. This deficiency is very important for practical applications, since the stress state in the field is often anisotropic.

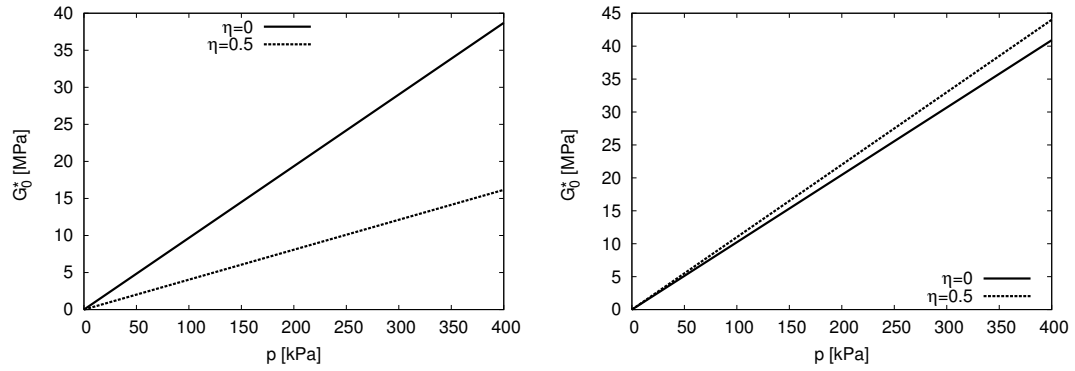

Figure 3. Influence of the stress ratio η on the hypoelastic shear modulus G_0^* calculated by the HK (left) and proposed (right) models with intergranular strains.

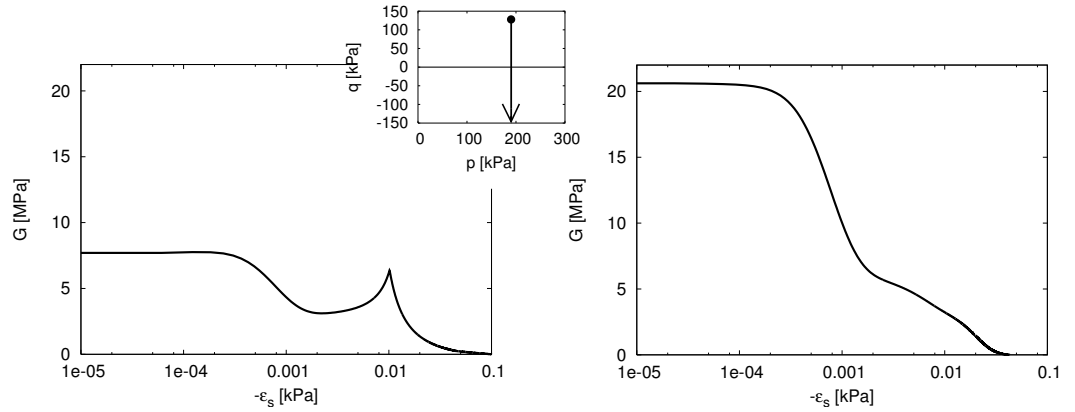

Figure 4. Erroneous increase of the shear stiffness calculated by the HK model enhanced by the intergranular strain concept for the stress path passing isotropic stress state (left) and corresponding predictions by the proposed model with intergranular strains (right).

Using the intergranular strain concept (Sec. 2.3), the quasi–elastic behaviour is controlled by the equation

$$\mathring{\mathbf{T}} = m_R f_s \boldsymbol{\mathcal{L}} : \mathbf{D}. \tag{46}$$

In the following, we restrict our attention only to axisymmetric conditions, as we want to examine possibility of calibration of model parameters, not to provide a full analysis of model performance. We may define the shear modulus G^* using Roscoe's variables p, q, ϵ_v and ϵ_s (e.g., [29]) as follows [11]:

$$\begin{bmatrix} \dot{p} \\ \dot{q} \end{bmatrix} = \begin{bmatrix} K^* & J \\ J & 3G^* \end{bmatrix} \begin{bmatrix} \dot{\epsilon_v} \\ \dot{\epsilon_s} \end{bmatrix}. \tag{47}$$

Because the hypoelastic stiffness tensor $\boldsymbol{\mathcal{L}}$ is not isotropic, G^* is equal to the equivalent shear modulus defined by $G = \dot{q}/(3\dot{\epsilon_s})$ only for undrained conditions.

Combining (46) and (47) we find that

$$G_0^* = \frac{m_R f_s}{3}\left[\mathcal{L}_{1111} - 2\mathcal{L}_{2211} + \frac{1}{2}\left(\mathcal{L}_{2222} + \mathcal{L}_{2233}\right)\right]. \tag{48}$$

Substituting expressions for $\boldsymbol{\mathcal{L}}$ (15) and f_s (32) we get

$$G_0^* = \frac{m_R p}{3\lambda^*\left(3 + a^2 - 2^\alpha a\sqrt{3}\right)}\left[\frac{27}{2}c_1 + \frac{c_2 a^2}{p^2}\left(T_{11}^2 - 2T_{22}T_{11} + \frac{1}{2}T_{22}^2 + \frac{1}{2}T_{22}T_{33}\right)\right], \tag{49}$$

and therefore

$$G_0^* = \frac{m_R p}{3\lambda^*\left(3 + a^2 - 2^\alpha a\sqrt{3}\right)}\left(\frac{27}{2}c_1 + c_2 a^2 \eta^2\right). \tag{50}$$

Eq. (50) shows that the modulus G_0^* predicted by the proposed model depends both on the mean stress p and stress ratio η. The second term in parenthesis in (50) is however significantly smaller, than the first term (for parameters derived in Sec. 6 and $\eta = 0.5$ the first term is 13.2 times larger). Therefore, contrary to the HK model, the influence of η on G_0^* is not significant. This observation is shown in Fig. 3 (right), with predictions by the HK model in Fig. 3 (left) for comparison. This drawback of the formulation of HK model is also demonstrated in Fig. 4 (left). The initial stiffness for the stress path, which starts at anisotropic stress state and passes isotropic stress state, is underpredicted and the model predicts unrealistic increase of the tangent stiffness at isotropic conditions. The improved prediction by the proposed model is in Fig. 4 (right).

As follows from Fig. 3 (right), for stress states with lower stress ratios η we can neglect the second term in (50) and write

$$G_0^* \simeq \frac{9 m_R c_1}{2\lambda^*\left(3 + a^2 - 2^\alpha a\sqrt{3}\right)} p, \tag{51}$$

and after substituting the expression for c_1 (45) we get the final simple form

$$G_0^* \simeq \frac{m_R}{r\lambda^*} p. \tag{52}$$

The shear modulus G_0^* may be measured by means of an undrained shear test[‡] in a triaxial apparatus equipped with high–accuracy local strain transducers (e.g., LVDT transducers [10]). However, because accurate quasi–static measurements of the shear stiffness are problematic, it is useful to derive an expression for the *out–of–axis* shear modulus G_0^{vh} [38, 22, 5, 23] (upper index v stands for *vertical* and h for *horizontal* direction), which can be measured by dynamic stiffness measurements (e.g., bender element tests [16]). Because

$$G_0^{vh} = \frac{m_R f_s}{2}\mathcal{L}_{1212}, \tag{53}$$

we find, after substituting expressions for $\boldsymbol{\mathcal{L}}$ (15), f_s (32) and c_1 (45), that

$$G_0^{vh} = \frac{m_R}{r\lambda^*} p. \tag{54}$$

[‡]In the context of this paper, the term "shear tests" is used for various types of axisymmetric loading tests performed in a triaxial cell, not in simple or torsional shear apparatuses.

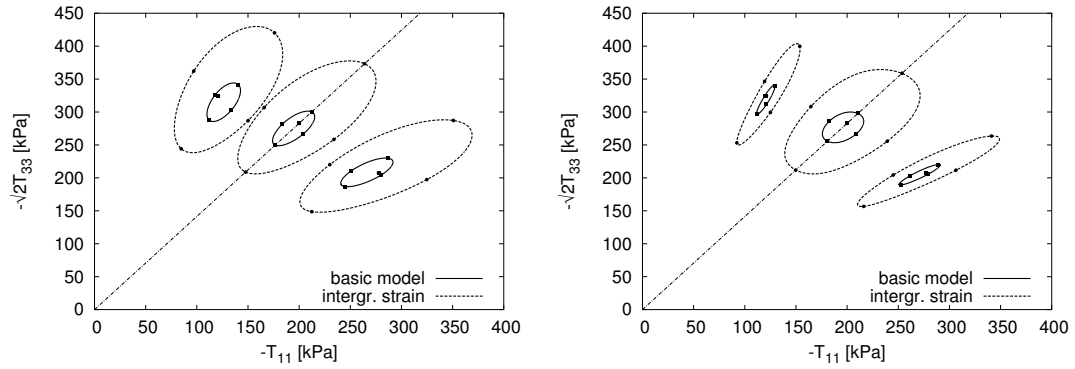

Figure 5. Response envelopes of the proposed model (left) and HK model (right) with and without intergranular strains for isotropic stress states and for $\varphi_{mob} = 18^\circ$ (with $\varphi_c = 22.6^\circ$) in triaxial compression and extension.

Therefore, at axisymmetric conditions the proposed model predicts a linear dependency of the initial shear modulus G_0^{vh} on the mean stress p, which is approximately correct (e.g. [44, 41]). Eq. (54) is valuable for the calibration of the parameter m_R, as discussed in Sec. 6.

In the previous paragraph we demonstrated that the initial shear stiffness in the "quasi–elastic" range of the proposed model is practically independent of the stress ratio η. Nevertheless, the shear stiffness for *intergranular swept–out–memory* states [32] (and the shear stiffness of the basic model without intergranular strain concept) must vanish as the stress approaches Matsuoka–Nakai states. This property of the proposed model can be studied using response envelopes (Fig. 5 (left)). It is evident that the response envelopes of the model with intergranular strain are centered about the reference stress point. On the other hand, for larger φ_{mob} the response envelopes of the basic model are significantly translated (ultimately, at Matsuoka–Nakai limit state they touch the reference stress point). It is also worth noting that the response envelopes do not change their shape substantially as the stress approaches the critical state. This is not the case for the HK model (Fig. 5 (right)), where the response envelopes for larger φ_{mob} become narrower. Note that also the VW hypoplastic model for granular materials retains similar shapes[§] of response envelopes for different φ_{mob}.

5.2. Stress–dilatancy behaviour

In this section we will study the influence of the novel expression for the pyknotropy factor f_d. Since a detailed study on the shape of the state boundary surface of the proposed constitutive model, defined as a boundary of all admissible states in the stress–porosity space, is presented in a forthcoming paper [26], we will restrict our attention to the shape of stress paths normalized

[§]Only the size of response envelopes decreases slightly, due to the factor $1/(\hat{\mathbf{T}} : \hat{\mathbf{T}})$ in the expression for $\boldsymbol{\mathcal{L}}$ (Sec. 4.1).

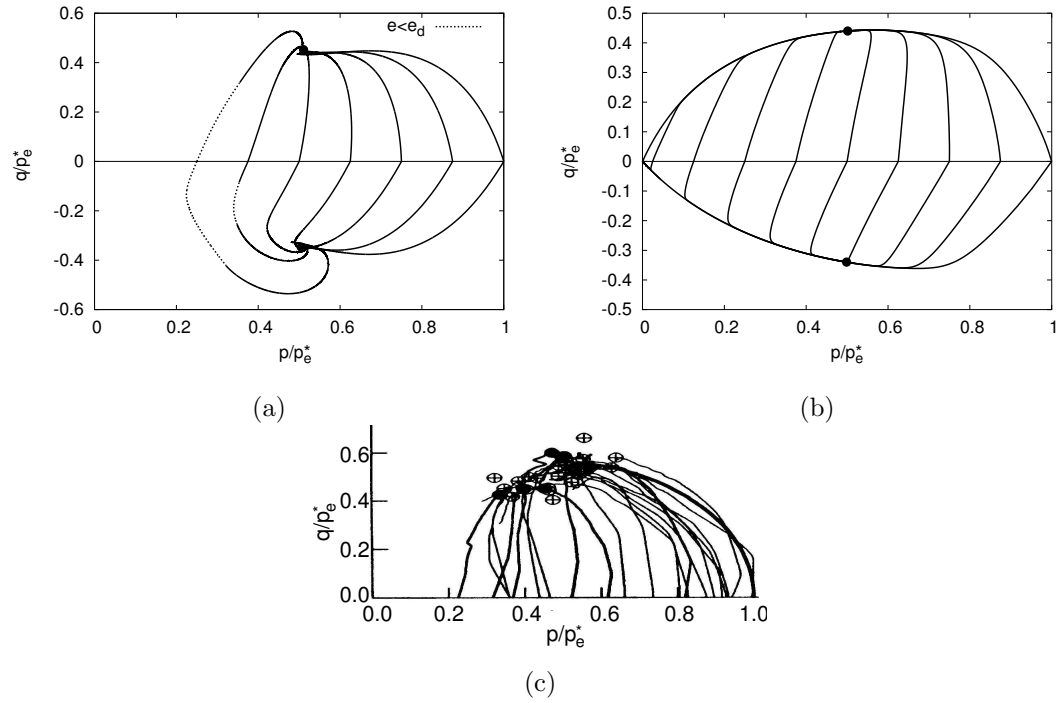

Figure 6. Normalized stress paths of drained shear tests calculated by the HK (a) and proposed (b) models, with critical states indicated by points. Experimental results by Rampello and Callisto [35] on natural Pisa clay for qualitative comparison (c). Simulations were performed with e = const., $q = 0$ kPa and varying p.

by the equivalent pressure at the isotropic normal compression line p_e^* [15] (Fig. 2), defined by

$$p_e^* = \exp\left\{\frac{N - \ln(1+e)}{\lambda^*}\right\}. \tag{55}$$

They are shown for drained triaxial tests in Fig. 6 (b), experimental results on natural Pisa clay [35] are given in Fig. 6 (c) for qualitative comparison. The proposed model predicts correctly dilatant/contractant behaviour for a wide range of overconsolidation ratios, down to $p = 0$. The increase in the peak friction angle for states *dry of critical* (defined by $p < p_{cr}$ or $p/p_e^* < 0.5$) is also evident.

Predictions by the HK model are shown for comparison in Fig. 6 (a). This figure reveals another shortcoming of the HK (VW) model, discussed by Niemunis et al. [34]. This model allows the lower limit of void ratio e_d to be surpassed. The parts of the stress paths, which pass inadmissible state $e < e_d$, are plotted using dotted lines in Fig. 6 (a)¶. It is clear that unlike the proposed model the HK model is not suitable for modelling clays with higher overconsolidation

¶Note that the factor f_d of the HK model is a complex number for $e < e_d$. In order to perform analyses, $f_d = 0$ for $e < e_d$ was prescribed, so predictions were for these states hypoelastic.

ratios.

5.3. Limitations of the proposed model

After sumarising the main advantages of the proposed model, let us now point out its limitations.

A particular form of barotropy and pyknotropy factors f_s and f_d prescribe constant shape and size of the state boundary surface (see [26] for detailed explanation). Therefore, the model is suitable for modeling reconstituted clays and natural clays with "stable" structure (constant sensitivity, in a sense defined in [9]). Its application to soft natural clays requires further development.

The aim of the work is to provide a practical engineering model with a minimal number of parameters, which may be evaluated on the basis of standard laboratory experiments. This fact certainly restricts freedom for calibration, which may be found to be limiting for certain non–standard geotechnical applications. In such a case, the proposed model may be used as a basis for further modifications.

6. DETERMINATION OF PARAMETERS

The model is evaluated on the basis of laboratory tests on reconstituted London clay (Mašín [25, 27]). These were performed in computer controlled triaxial apparatuses. In addition to the standard equipment, three local submersible LVDT transducers RDP D5/200 [10] and a pair of bender elements [16] were used in order to study also the behaviour in the small strain range.

Parameters N, λ^* and κ^*: These parameters were calibrated on the basis of a single isotropic loading/unloading test (Fig. 7 left). Isotropic loading must exceed preconsolidation pressure in order to find the position and the slope of the normal compression line. Parameter κ^* should be calibrated from the slope of the isotropic unloading line close to the normally compressed state[‖].

Parameter φ_c: The critical state friction angle was found using a linear regression through the critical state points of all shear tests available.

Parameter r: Parameter r may be evaluated directly, using the definition (Sec. 4.6), as a ratio of the bulk and shear moduli for tests starting from isotropic normally compressed stress state. However, since the model predicts gradual degradation of the shear stiffness, it is advisable to find an appropriate value of the parameter r by a parametric study. This approach is acceptable because there is no interrelation with other model parameters, which would require parametric study for calibration.

[‖] Note that the proposed model is formulated in such a way that the slope of the predicted isotropic unloading line in $\ln(1+e) : \ln p$ space is exactly equal to parameter κ^* only for unloading from normally compressed state.

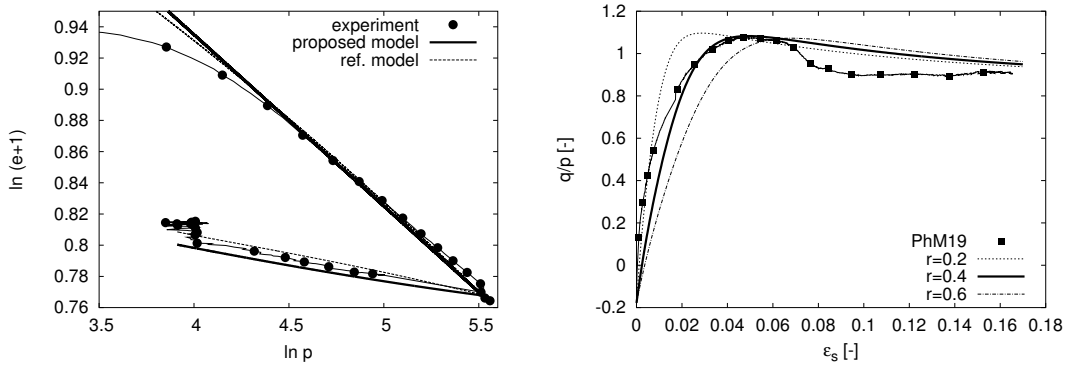

Figure 7. Calibration of parameters N, λ^* and κ^* on the basis of isotropic loading and unloading test. Unlike the experiment, simulation started from normally compressed state (left). Calibration of parameter r using a parametric study (right).

Table I. Summary of parameters of the basic version of the proposed model (left) and of the intergranular strain extension (right) for London clay. Standard values may be assumed for parameters in parenthesis

φ_c [°]	λ^*	κ^*	N	r
22.6	0.11	0.016	1.375	0.4

m_R	(m_T)	(R)	(β_r)	(χ)
4.5	(4.5)	(10^{-4})	(0.2)	(6)

The parameter r was calibrated on the basis of the stress–strain curve of the shear test with constant mean pressure on K_0 overconsolidated specimen (PhM19), Fig. 7 (right).

Parameters for the small strain range (intergranular strain concept): Intergranular strain concept (Sec. 2.3) requires five additional model parameters. Their calibration is described in the original paper [32]. Experience however shows that three of these parameters have similar values for a broad range of different soils and without suitable laboratory experiments we can assume "standard" values: $R = 10^{-4}$, $\beta_r = 0.2$ and $\chi = 6$. Due to the lack of suitable laboratory experiments we also assume $m_T = m_R$.

The parameter m_R may be conveniently calibrated on the basis of the shear stiffness measurements with bender elements using Eq. (54). Knowing the values of parameters λ^* and r we use a linear regression in $G_0^{vh} : p$ space and from the slope calculate the value of parameter m_R, as shown in Figure 8.

Derived parameters of the proposed model for London clay are given in Table I.

6.1. Calibration of the HK model

The HK model was calibrated on the basis of the same laboratory tests as the proposed model to compare their predictions. Parameters h_s, n and e_{i0}, which define the position and the shape of the isotropic normal compression line, were calibrated using isotropic compression test depicted in Fig. 7 (left). An isotropic unloading test was used to calibrate parameters α and β. Because a direct calibration is difficult, parameters α and β were derived by means of

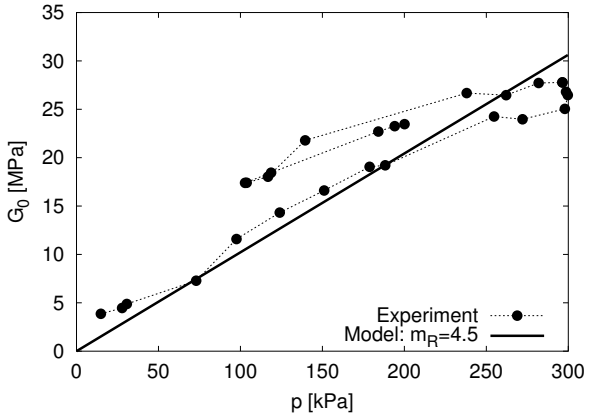

Figure 8. Calibration of parameter m_R using linear regression on results from bender element tests.

Table II. Summary of parameters of the basic version of the HK model for London clay.

ϕ_c [°]	h_s [kPa]	n	e_{d0}	e_{c0}	e_{i0}	α	β	r
22.6	659	0.214	2.6	2.8	3.23	0.45	2	0.6

a parametric study. It may be seen from Fig. 7 (left) that correctly chosen parameters allow similar predictions of the isotropic test by both the HK and the proposed model (in the chosen stress range). The advantage of the proposed model is the smaller number of parameters, which all have a well defined physical meaning.

The parameter e_{c0} was calibrated by fitting the position of the critical state line in $p:e$ space. The calculation of the parameter e_{d0} from the water content at the plastic limit, as suggested in [14], leads to incorrect predictions of dilatant/contractant behaviour of overconsolidated specimens. The calibration of e_{d0} was therefore based on the correct predictions of dilatant behaviour of an overconsolidated specimen (PhM19). Finally, the parameter r was evaluated using a parametric study on a stress–strain curve of the test PhM19. The numerical value of the parameter r is different compared to the proposed model, due to slightly different expressions for scalar factor c_1, see Appendixes A and C**. The HK model does not allow direct evaluation of the parameter m_R using $G_0:p$ curve. Small strain parameters of the proposed model were therefore assumed also for the HK model. Parameters of the HK model are summarized in Table II.

**In the formulation of the HK model, the expression for f_{di} is omitted in the calculation of the scalar factor c_1

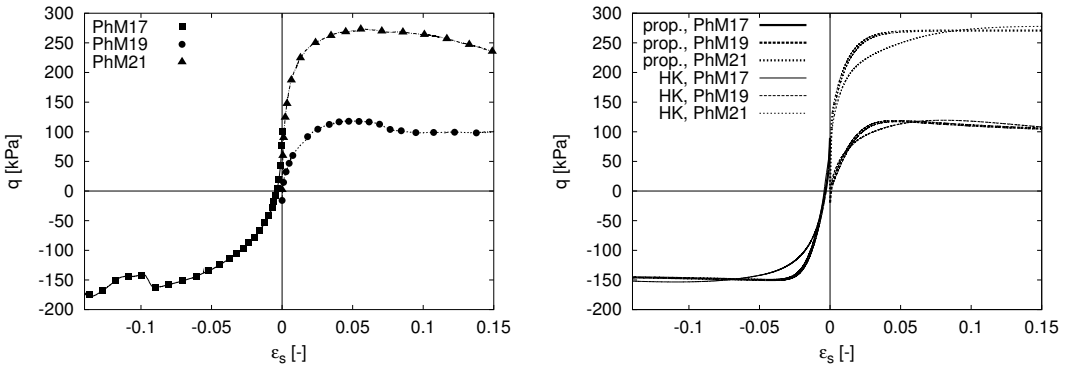

Figure 9. Stress–strain curves of three different compression tests. Experimental (left) and simulated (right). Simulation by the basic versions of the HK and proposed model.

7. MODEL PREDICTIONS

An extensive evaluation of the predictions by the proposed model, compared with different elasto–plastic and hypoplastic models, is presented in a forthcoming paper [28]. In this work, we simulate laboratory experiments, which were not used to calibrate the constitutive model[††], in order to demonstrate the capability of the model to predict different aspects of the clay behaviour. The basic version of the model is mostly used, the intergranular strain concept is adopted only when the behaviour at small strains is important.

Two other shear tests in addition to the test PhM19 were simulated. An undrained compression test on a nearly normally compressed specimen (PhM21) and a constant p' extension test on a K_0 overconsolidated specimen (PhM17). The experimental and simulated stress–strain curves are shown in Fig. 9. To assess volumetric changes in drained tests and development of pore pressures in undrained tests, it is useful to study the shape of stress paths normalized with respect to the equivalent pressure p_e^*, shown in Fig. 10.

Comparisons of predictions by the HK and proposed model in Figs. 9 and 10 indicate that for soils with medium overconsolidation ratios the predictions of the shear behaviour at large strains are similar. In this case the proposed model has the advantage of a simpler calibration. For higher overconsolidation ratios however, large–strain predictions by both models differ significantly due to the different formulation of the pyknotropy factor f_d (Fig. 6).

Since stiffness at small strains was measured by means of local LVDT transducers, we can study also the capability of the models to predict degradation of the shear stiffness in the small strain range, Fig. 11. The proposed model (Fig. 11 (b)) predicts correctly initial shear modulus and degradation of stiffness for tests PhM17 and PhM19, although the test PhM17 started from an anisotropic stress state (Fig. 10). The initial stiffness of the test PhM21 is slightly overpredicted. This comes from the fact that the test PhM21 was performed at a larger mean stress (450 kPa) than the stress range used for calibration of the parameter m_R (Fig. 8). Predictions by the HK model (Fig. 11 (a)) are comparable with predictions by the

[††]Except for parameter φ_c

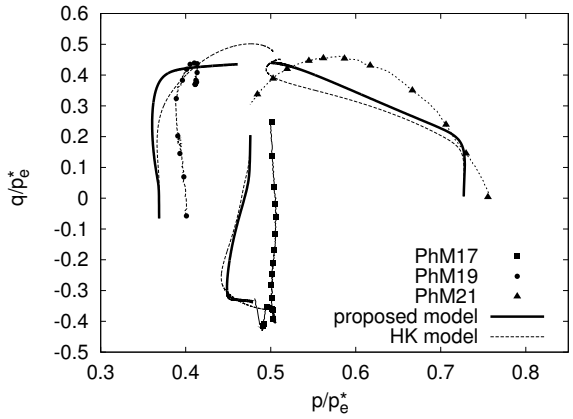

Figure 10. Normalised stress paths of three shear tests. Simulation by the HK and proposed models, both extended with the intergranular strain concept.

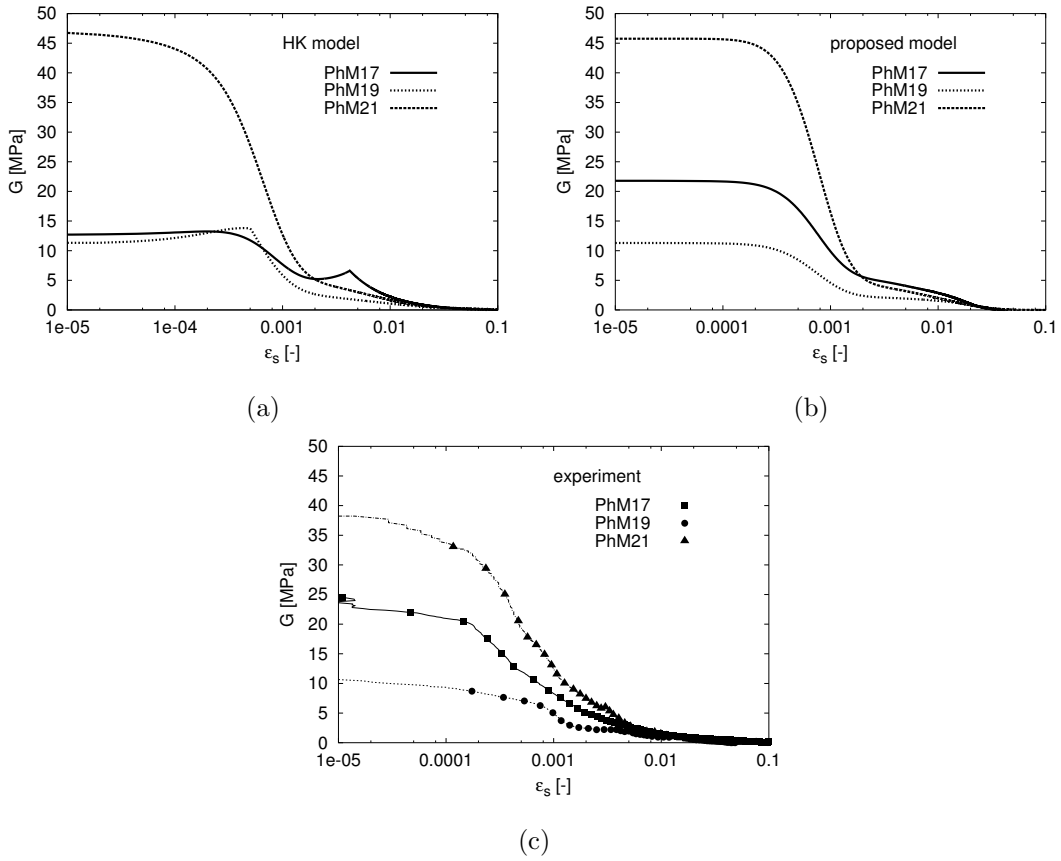

Figure 11. Degradation of the tangent shear stiffness at small strains. Simulation by the HK (a) and proposed (b) model, both enhanced by the intergranular strain concept, and experimental results (c).

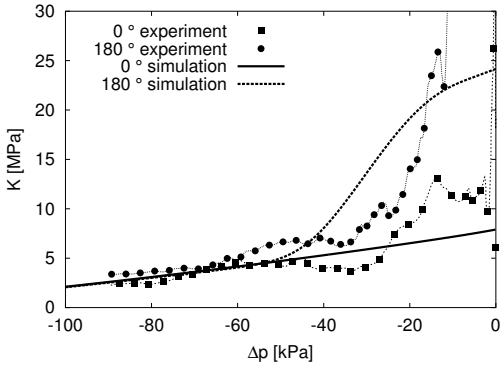

Figure 12. Variation of bulk modulus in the isotropic unloading test with different degrees of strain path rotation. Experiment and simulation by the proposed model with intergranular strains.

proposed model only for the test PhM21, which started from the nearly isotropic stress state. The initial stiffness of the test PhM17, with the anisotropic initial stress state, is significantly underpredicted and the HK model simulates an incorrect increase of the shear stiffness at larger shear strains.

One isotropic loading/unloading test was performed with two different degrees of strain path rotation (0° and 180°) starting from the same mean stress and overconsolidation ratio. Experimental variation of the bulk moduli and simulations by the proposed model are shown in Fig. 12. The experimental data show a marked scatter and the model predicts correctly the trend. Satisfactory predictions were achieved although the parameter m_R was calibrated only on the basis of dynamic measurements of the *shear* stiffness.

8. CONCLUSIONS

This paper has presented a new hypoplastic constitutive model for clays. The model uses a formulation of the generalised hypoplasticity [31], which allows independent treatment of different aspects of soil behaviour. In this way it was possible to develop a model particularly suitable for fine–grained soils.

The proposed model combines hypoplasticity principles with the traditional critical state soil mechanics. Parameters required by the model correspond to the parameters of the Modified Cam clay model and are simple to calibrate on the basis of standard laboratory tests, which makes the model particularly suitable for practical applications.

The model has been developed to predict soil behaviour at larger strains. However, it may be enhanced simply by the intergranular strain concept [32] to allow predictions to also be made at small to very small strains. The calibration of additional parameters, which are related to the parameters of the basic model, have also been discussed briefly in the paper.

The model is evaluated on the basis of high quality laboratory measurements on reconstituted specimens of London clay. It is demonstrated that with a minimal number of parameters the model is capable of predicting a wide range of aspects of fine grained soils behaviour. Apart from the advantage of simpler calibration, the proposed model significantly

improves predictions of the HK model [14] for clays with higher overconsolidation ratios and predictions of the behaviour in the small–strain range at anisotropic stress states.

ACKNOWLEDGEMENT

The author is grateful to Prof. I. Herle and Prof. D. Kolymbas for stimulating discussions and valuable remarks on the manuscript and to Dr. S. E. Stallebrass and Prof. J. H. Atkinson for enabling him to carry out the laboratory experiments at City University, London. The financial support by the research grant GACR 205/03/1467 is gratefully appreciated.

APPENDIX A

This appendix summarizes mathematical formulation of a hypoplastic model for soils with low friction angles by Herle and Kolymbas [14].

The model assumes the following stress–strain relation:

$$\mathring{\mathbf{T}} = f_s \boldsymbol{\mathcal{L}} : \mathbf{D} + f_s f_d \mathbf{N} \|\mathbf{D}\|, \tag{56}$$

with

$$\boldsymbol{\mathcal{L}} = \frac{1}{\hat{\mathbf{T}} : \hat{\mathbf{T}}} \left(c_1 F^2 \boldsymbol{\mathcal{I}} + c_2 a^2 \hat{\mathbf{T}} \otimes \hat{\mathbf{T}} \right), \tag{57}$$

$$\mathbf{N} = \frac{Fa}{\hat{\mathbf{T}} : \hat{\mathbf{T}}} \left(\hat{\mathbf{T}} + \hat{\mathbf{T}}^* \right), \tag{58}$$

where $\mathbf{1}$ is a second–order unity tensor, $\mathcal{I}_{ijkl} = \frac{1}{2}\left(1_{ik}1_{jl} + 1_{il}1_{jk}\right)$ is a fourth-order unity tensor and

$$\mathrm{tr}\mathbf{T} = \mathbf{T} : \mathbf{1}, \qquad \hat{\mathbf{T}} = \mathbf{T}/\mathrm{tr}\mathbf{T}, \qquad \hat{\mathbf{T}}^* = \hat{\mathbf{T}} - \mathbf{1}/3, \tag{59}$$

$$a = \frac{\sqrt{3}\,(3 - \sin\varphi_c)}{2\sqrt{2}\sin\varphi_c}, \qquad F = \sqrt{\frac{1}{8}\tan^2\psi + \frac{2 - \tan^2\psi}{2 + \sqrt{2}\tan\psi\cos 3\theta}} - \frac{1}{2\sqrt{2}}\tan\psi, \tag{60}$$

with

$$\tan\psi = \sqrt{3}\|\hat{\mathbf{T}}^*\|, \qquad \cos 3\theta = -\sqrt{6}, \frac{\mathrm{tr}\left(\hat{\mathbf{T}}^* \cdot \hat{\mathbf{T}}^* \cdot \hat{\mathbf{T}}^*\right)}{\left[\hat{\mathbf{T}}^* : \hat{\mathbf{T}}^*\right]^{3/2}}. \tag{61}$$

The scalar factors f_s and f_d take into account the influence of mean pressure and density,

$$f_s = \frac{h_s}{n}\left(\frac{e_i}{e}\right)^{\beta} \frac{1 + e_i}{e}\left(\frac{-\mathrm{tr}\mathbf{T}}{h_s}\right)^{1-n}\left[3c_1 + a^2 c_2 - a\sqrt{3}\left(\frac{e_{i0} - e_{d0}}{e_{c0} - e_{d0}}\right)^{\alpha}\right]^{-1}, \tag{62}$$

$$f_d = \left(\frac{e - e_d}{e_c - e_d}\right)^{\alpha}. \tag{63}$$

The characteristic void ratios – e_i, e_c and e_d decrease with the mean pressure according to the relation

$$\frac{e_i}{e_{i0}} = \frac{e_c}{e_{c0}} = \frac{e_d}{e_{d0}} = \exp\left[-\left(\frac{-\mathrm{tr}\mathbf{T}}{h_s}\right)^n\right]. \tag{64}$$

The scalar factors c_1 and c_2 are calculated using

$$c_1 = \left(\frac{1 + \frac{1}{3}a^2 - \frac{1}{\sqrt{3}}a}{1.5r}\right)^{\xi}, \tag{65}$$

$$c_2 = 1 + (1 - c_1)\,\frac{3}{a^2}, \tag{66}$$

$$\xi = \left\langle \frac{\sin\varphi_c - \sin\varphi_{mob}}{\sin\varphi_c} \right\rangle, \qquad \text{where} \qquad \sin\varphi_{mob} = \frac{T_1 - T_3}{T_1 + T_3}. \tag{67}$$

T_1 and T_3 are the maximal and minimal principal stresses, φ_{mob} is a mobilized friction angle and $\langle\rangle$ are Macauley brackets: $\langle x\rangle = (x + |x|)/2$.

The model requires 9 parameters: ϕ_c, h_s, n, e_{d0}, e_{c0}, e_{i0}, α, β and r.

APPENDIX B

To capture correctly behaviour in the small to very small strain range the hypoplastic model must be enhanced by the intergranular strain concept [32].

In the extended hypoplastic model the strain is considered as a result of deformation of the intergranular interface layer and of rearrangement of the skeleton. The interface deformation is called *intergranular strain* $\boldsymbol{\delta}$ and is considered as a new tensorial state variable ($\boldsymbol{\delta}$ is a symmetric second–order tensor). It is convenient to denote the normalized magnitude of $\boldsymbol{\delta}$ as

$$\rho = \frac{\|\boldsymbol{\delta}\|}{R}, \tag{68}$$

and the direction $\hat{\boldsymbol{\delta}}$ of the intergranular strain as

$$\hat{\boldsymbol{\delta}} = \begin{cases} \boldsymbol{\delta}/\|\boldsymbol{\delta}\|, & \text{for } \boldsymbol{\delta} \neq \mathbf{0}; \\ \mathbf{0}, & \text{for } \boldsymbol{\delta} = \mathbf{0}. \end{cases} \tag{69}$$

The general stress–strain relation is now written as

$$\mathring{\mathbf{T}} = \boldsymbol{\mathcal{M}} : \mathbf{D}. \tag{70}$$

The fourth-order tensor $\boldsymbol{\mathcal{M}}$ represents stiffness and is calculated from the hypoplastic tensors $\boldsymbol{\mathcal{L}}$ and $\mathbf{N}$ and a function of the intergranular strain using the following interpolation:

$$\boldsymbol{\mathcal{M}} = \left[\rho^{\chi} m_T + (1 - \rho^{\chi})\, m_R\right] f_s \boldsymbol{\mathcal{L}} + \begin{cases} \rho^{\chi}\,(1 - m_T)\, f_s \boldsymbol{\mathcal{L}} : \hat{\boldsymbol{\delta}} \otimes \hat{\boldsymbol{\delta}} + \rho^{\chi} f_s f_d \mathbf{N}\hat{\boldsymbol{\delta}}, & \text{for } \hat{\boldsymbol{\delta}} : \mathbf{D} > 0; \\ \rho^{\chi}\,(m_R - m_T)\, f_s \boldsymbol{\mathcal{L}} : \hat{\boldsymbol{\delta}} \otimes \hat{\boldsymbol{\delta}}, & \text{for } \hat{\boldsymbol{\delta}} : \mathbf{D} \leq 0. \end{cases} \tag{71}$$

The evolution equation for the intergranular strain tensor $\boldsymbol{\delta}$ is governed by

$$\mathring{\boldsymbol{\delta}} = \begin{cases} \left(\boldsymbol{\mathcal{I}} - \hat{\boldsymbol{\delta}} \otimes \hat{\boldsymbol{\delta}} \rho^{\beta_r}\right) : \mathbf{D}, & \text{for } \hat{\boldsymbol{\delta}} : \mathbf{D} > 0; \\ \mathbf{D}, & \text{for } \hat{\boldsymbol{\delta}} : \mathbf{D} \leq 0. \end{cases} \tag{72}$$

where $\mathring{\boldsymbol{\delta}}$ is the objective rate of intergranular strain. The hypoplastic model with intergranular strains requires five additional model parameters: R, m_R, m_T, β_r and χ.

APPENDIX C

Mathematical formulation of the proposed hypoplastic constitutive model for clays:

The general stress–strain relation reads

$$\mathring{\mathbf{T}} = f_s \boldsymbol{\mathcal{L}} : \mathbf{D} + f_s f_d \mathbf{N} \|\mathbf{D}\|, \tag{73}$$

with

$$\mathbf{N} = \boldsymbol{\mathcal{L}} : \left(-Y \frac{\mathbf{m}}{\|\mathbf{m}\|}\right). \tag{74}$$

The hypoelastic tensor $\boldsymbol{\mathcal{L}}$ is

$$\boldsymbol{\mathcal{L}} = 3\left(c_1 \boldsymbol{\mathcal{I}} + c_2 a^2 \hat{\mathbf{T}} \otimes \hat{\mathbf{T}}\right), \tag{75}$$

where $\mathbf{1}$ is a second–order unity tensor, $\mathcal{I}_{ijkl} = \frac{1}{2}\left(1_{ik}1_{jl} + 1_{il}1_{jk}\right)$ is a fourth-order unity tensor and

$$\mathrm{tr}\mathbf{T} = \mathbf{T} : \mathbf{1}, \qquad \hat{\mathbf{T}} = \mathbf{T}/\mathrm{tr}\mathbf{T}, \qquad \hat{\mathbf{T}}^* = \hat{\mathbf{T}} - \mathbf{1}/3, \tag{76}$$

$$a = \frac{\sqrt{3}\left(3 - \sin\varphi_c\right)}{2\sqrt{2}\sin\varphi_c}. \tag{77}$$

The degree of nonlinearity Y, with the limit value $Y = 1$ at Matsuoka–Nakai failure surface, is calculated by

$$Y = \left(\frac{\sqrt{3}a}{3 + a^2} - 1\right) \frac{\left(I_1 I_2 + 9 I_3\right)\left(1 - \sin^2\varphi_c\right)}{8 I_3 \sin^2\varphi_c} + \frac{\sqrt{3}a}{3 + a^2}, \tag{78}$$

with stress invariants I_1, I_2 and I_3,

$$I_1 = \mathrm{tr}\mathbf{T}, \qquad I_2 = \frac{1}{2}\left[\mathbf{T} : \mathbf{T} - \left(I_1\right)^2\right], \qquad I_3 = \det\mathbf{T}. \tag{79}$$

The tensorial quantity $\mathbf{m}$ defining the hypoplastic flow rule has the following formulation:

$$\mathbf{m} = -\frac{a}{F}\left[\hat{\mathbf{T}} + \hat{\mathbf{T}}^* - \frac{\hat{\mathbf{T}}}{3}\left(\frac{6\ \hat{\mathbf{T}} : \hat{\mathbf{T}} - 1}{\left(F/a\right)^2 + \hat{\mathbf{T}} : \hat{\mathbf{T}}}\right)\right], \tag{80}$$

with factor F given by

$$F = \sqrt{\frac{1}{8}\tan^2\psi + \frac{2 - \tan^2\psi}{2 + \sqrt{2}\tan\psi\cos 3\theta}} - \frac{1}{2\sqrt{2}}\tan\psi, \tag{81}$$

where

$$\tan\psi = \sqrt{3}\|\hat{\mathbf{T}}^*\|, \qquad \cos 3\theta = -\sqrt{6}\frac{\mathrm{tr}\left(\hat{\mathbf{T}}^* \cdot \hat{\mathbf{T}}^* \cdot \hat{\mathbf{T}}^*\right)}{\left[\hat{\mathbf{T}}^* : \hat{\mathbf{T}}^*\right]^{3/2}}. \tag{82}$$

Barotropy and pyknotropy factors f_s and f_d read

$$f_s = -\frac{\mathrm{tr}\mathbf{T}}{\lambda^*}\left(3 + a^2 - 2^\alpha a\sqrt{3}\right)^{-1}, \qquad f_d = \left[-\frac{2\mathrm{tr}\mathbf{T}}{3p_r}\exp\left(\frac{\ln(1+e) - N}{\lambda^*}\right)\right]^\alpha, \tag{83}$$

where p_r is the reference stress 1 kPa and the scalar quantity α is calculated by

$$\alpha = \frac{1}{\ln 2}\ln\left[\frac{\lambda^* - \kappa^*}{\lambda^* + \kappa^*}\left(\frac{3 + a^2}{a\sqrt{3}}\right)\right]. \tag{84}$$

Finally, factors c_1 and c_2 are calculated as follows:

$$c_1 = \frac{2\left(3 + a^2 - 2^\alpha a\sqrt{3}\right)}{9r}, \qquad c_2 = 1 + (1 - c_1)\frac{3}{a^2}. \tag{85}$$

The model requires five constitutive parameters: φ_c, λ^*, κ^*, N and r.

REFERENCES

1. Bauer E. Calibration of a comprehensive hypoplastic model for granular materials. *Soils and Foundations* 1996; **36**(1):13–26.
2. Butterfield R. A natural compression law for soils. *Géotechnique* 1979; **29**(4):469–480.
3. Callisto L, Calabresi G. Mechanical behaviour of a natural soft clay. *Géotechnique* 1998; **48**(4):495–513.
4. Callisto L, Rampello S. Shear strength and small–strain stiffness of a natural clay under general stress conditions. *Géotechnique* 2002; **52**(8):547–560.
5. Chambon R. Discussion of paper "Shear and objective stress rates in hypoplasticity" by D. Kolymbas and I. Herle. *International Journal for Numerical and Analytical Methods in Geomechanics* 2004; **28**:365–372.
6. Chambon R, Desrues J, Hammad W, Charlier R. CLoE, a new rate–type constitutive model for geomaterials: theoretical basis and implementation. *International Journal for Numerical and Analytical Methods in Geomechanics* 1994; **18**:253–278.
7. Cotecchia F. *The effects of structure on the properties of an Italian Pleistocene clay.* PhD thesis, University of London, 1996.
8. Cotecchia F, Chandler J. The influence of structure on the pre–failure behaviour of a natural clay. *Géotechnique* 1997; **47**(3):523–544.
9. Cotecchia F, Chandler J. A general framework for the mechanical behaviour of clays. *Géotechnique* 2000; **50**(4):431–447.
10. Cuccovillo T, Coop MR. The measurement of local axial strains in tiaxial tests using LVDT's. *Géotechnique* 1997; **47**(1):167–171.
11. Graham J, Houlsby GT. Anisotropic elasticity of a natural clay. *Géotechnique* 1983; **33**(2):165–180.
12. Gudehus G. A comparison of some constitutive laws for soils under radially symmetric loading and unloading. In *Proc. 3rd Int. Conf. on Numerical Methods in Geomechanics,* Aachen, 1979; 1309-1323.
13. Gudehus G. A comprehensive constitutive equation for granular materials. *Soils and Foundations* 1996; **36**(1):1–12.
14. Herle I, Kolymbas D. Hypoplasticity for soils with low friction angles. *Computers and Geotechnics* 2004; **31**:365–373.
15. Hvorslev M. Physical components of the shear strength of saturated clays. In *Shear Strength of Cohesive Soils, proc. ASCE Research Conf.,* Boulder, Colorado, 1960.
16. Jovičić V. *The measurement and interpretation of small strain stiffness of soil.* PhD thesis, City University, London, 1997.

17. Jovičić V, Coop MR. The measurement of stiffness anisotropy in clays with bender element tests in the triaxial apparatus. *Geotechnical Testing Journal* 1993; **21**(1):3–10.
18. Kirkgard MM, Lade PV. Anisotropic three–dimensional behaviour of a normally consolidated clay. *Canadian Geotechnical Journal* 1993; **30**:848–858.
19. Kolymbas D. *Eine konstitutive Theorie für Böden und andere körnige Stoffe.* PhD thesis, University of Karlsruhe, 1978.
20. Kolymbas D. Computer-aided design of constitutive laws. *International Journal for Numerical and Analytical Methods in Geomechanics* 1991; **15**:593–604.
21. Kolymbas D. An outline of hypoplasticity. *Archive of Applied Mechanics* 1991; **61**:143–151.
22. Kolymbas D, Herle I. Shear and objective stress rates in hypoplasticity. *International Journal for Numerical and Analytical Methods in Geomechanics* 2004; **27**:733–744.
23. Lanier J, Caillerie D, Chambon R, Viggiani G, Bésuelle P, Desrues J. A general formulation of hypoplasticity. *International Journal for Numerical and Analytical Methods in Geomechanics* 2004; **28**(15):1461–1478.
24. Matsuoka H, Nakai T. Stress–deformation and strength characteristics of soil under three different principal stresses. In *Proc. Japanese Soc. of Civil Engineers,* 1974; **232**:59–70.
25. Mašín D. *Laboratory and numerical modelling of natural clays.* MPhil Thesis, City University, London, 2004.
26. Mašín D, Herle I. State boundary surface of a hypoplastic model for clays. *Computers and Geotechnics* 2005; Submitted for publication.
27. Mašín D, Stallebrass SE, Atkinson JH. Laboratory modelling of natural structured clays. In *Proc. International Workshop on Geotechnics of Soft Soils – Theory and Practice,* Noordwijkerhout, Netherlands, 2003; 253–263.
28. Mašín D, Tamagnini C, Viggiani G, Costanzo D. An evaluation of different constitutive models to predict the directional response of reconstituted fine–grained soil. In preparation.
29. Muir Wood D. *Soil behaviour and critical state soil mechanics.* Cambridge University Press, 1990.
30. Niemunis A. A visco–hypoplastic model for clay and its FE implementation. In *Resultats recents en mechanique des sols et des roches XI Colloque Franco-Polonais,* Gdańsk, 1996.
31. Niemunis A. *Extended hypoplastic model for soils.* Habilitation thesis, Ruhr-University, Bochum, 2002.
32. Niemunis A, Herle I. Hypoplastic model for cohesionless soils with elastic strain range. *Mechanics of Cohesive-Frictional Materials* 1997; **2**:279–299.
33. Niemunis A, Krieg S. Viscous behaviour of soil under oedometric conditions. *Canadian Geotechnical Journal* 1996; **33**:159–168.
34. Niemunis A, Nübel K, Karcher Ch. The consistency conditions for density limits of hypoplastic constitutive law. *Task Quarterly* 2000; **4**(3):412–420.
35. Rampello S, Callisto L. A study on the subsoil of the Tower of Pisa based on results from standard and high–quality samples. *Canadian Geotechnical Journal* 1998; **35**(6):1074–1092.
36. Roscoe KH, Burland JB. On the generalised stress-strain behaviour of wet clay. In *Engineering Plasticity,* Heyman J, Leckie FA (eds). Cambridge: Cambridge Univesrity Press, 1968; 535–609.
37. Schofield AN, Wroth CP. *Critical state soil mechanics* Mc–Graw–Hill, London.
38. Tamagnini C, Viggiani G, Chambon R. A review of two different approaches to hypoplasticity. In *Constitutive modelling of granular materials,* Kolymbas D (eds). Springer, 1999; 107–144.
39. Tamagnini C, Viggiani G, Chambon R, Desrues J. Evaluation of different strategies for the integration of hypoplastic constitutive equations. *Mechanics of Cohesive-Frictional Materials* 2000; **5**:263–289.
40. Teachavorasinskun S, Amornwithayalax T. Elastic shear modulus of Bangkok clay during undrained triaxial compression. *Géotechnique* 2002; **52**(7):537–540.
41. Viggiani G, Atkinson JH. Stiffness of fine–grained soil at very small strains. *Géotechnique* 1995; **45**(2):245–265.
42. Wang CC. A new representation theorem for isotropic tensor functions. *Archive for Rational Mechanics and Analysis* 1970; **36**:166–223.
43. von Wolffersdorff PA. A hypoplastic relation for granular materials with a predefined limit state surface. *Mechanics of Cohesive-Frictional Materials* 1996; **1**:251–271.
44. Wroth CP, Houlsby GT. Soil mechanics - property characterization, and analysis procedures. In *Proc.* 11^{th} *Conf. Soil. Mech.* San Francisco, 1985; 1–55.
45. Wu W. *Hypoplastizität als mathematisches Modell zum mechanischen Verhalten granularer Stoffe.* PhD thesis, University of Karlsruhe, 1992.
46. Wu W, Bauer E. A simple hypoplastic constitutive model for sand. *International Journal for Numerical and Analytical Methods in Geomechanics* 1994; **18**:833–862.

Preprint: Accepted for publication